Biochemistry and Biophysics Reports 8 (2016) 75–80

Contents lists available at ScienceDirect

Biochemistry and Biophysics Reports

journal homepage: www.elsevier.com/locate/bbrep

The effects of high concentrations of ionic liquid on GB1 protein structure and dynamics probed by high-resolution magic-angle-spinning NMR spectroscopy

Lisa Warner [a,1], Erica Gjersing [a], Shelby E. Follett [b], K. Wade Elliott [b], Sergei V. Dzyuba [c], Krisztina Varga [b,*]

[a] National Renewable Energy Laboratory, Golden, CO 80401, USA
[b] Department of Chemistry, University of Wyoming, Laramie, WY 82071, USA
[c] Department of Chemistry and Biochemistry, Texas Christian University, Fort Worth, TX 76129, USA

ARTICLE INFO

Article history:
Received 5 May 2016
Received in revised form
24 July 2016
Accepted 1 August 2016
Available online 11 August 2016

Keywords:
Imidazolium ionic liquid
GB1
Ionic liquid–protein interaction
HR-MAS NMR

ABSTRACT

Ionic liquids have great potential in biological applications and biocatalysis, as some ionic liquids can stabilize proteins and enhance enzyme activity, while others have the opposite effect. However, on the molecular level, probing ionic liquid interactions with proteins, especially in solutions containing high concentrations of ionic liquids, has been challenging. In the present work the ^{13}C, ^{15}N-enriched GB1 model protein was used to demonstrate applicability of high-resolution magic-angle-spinning (HR-MAS) NMR spectroscopy to investigate ionic liquid–protein interactions. Effect of an ionic liquid (1-butyl-3-methylimidazolium bromide, [C_4-mim]Br) on GB1was studied over a wide range of the ionic liquid concentrations (0.6–3.5 M, which corresponds to 10–60% v/v). Interactions between GB1 and [C_4-mim]Br were observed from changes in the chemical shifts of the protein backbone as well as the changes in ^{15}N ps-ns dynamics and rotational correlation times. Site-specific interactions between the protein and [C_4-mim]Br were assigned using 3D methods under HR-MAS conditions. Thus, HR-MAS NMR is a viable tool that could aid in elucidation of molecular mechanisms of ionic liquid–protein interactions.

1. Introduction

Ionic liquids are customizable materials that are composed entirely of ions and have phase transitions at or below room temperature. Ionic liquids provide a unique chemical environment and have drawn considerable attention in recent years, with numerous applications as media for chemical and biocatalytic transformations [1,2], preparation of materials [3–5], energy-related processes [6–8], as well as several environmental [9–11] and analytical [12,13] systems. Notably, many recent reports describe the ability of ionic liquids to modulate inter- and intramolecular interactions of small molecules [14–16].

The microenvironment surrounding a protein can greatly effect its folded state (including secondary and tertiary structure), stability, and function. Ionic liquids offer unique environments that can be tuned to alter the structural and biophysical properties of biomacromolecules. Thus, understanding the effect of ionic liquids on the native structure of biomacromolecules is a critical step in the advancement of many areas, including enzymology, biocatalysis, and bioengineering.

While it is evident that ionic liquids can alter the stability and function of proteins, the current mechanistic understanding of protein stability and enzyme activity in ionic liquid-rich environments requires clarification. For example, some ionic liquids were noted to increase the stability of proteins by serving as an anti-aggregation/unfolding media for lysozyme over an extended period of time [17]. However, it was also shown that certain proteins, for example the redox active form of cytochrome *c*, could be denatured by imidazolium-based ionic liquids [18,19], yet choline-based ionic liquids were recently shown to improve the redox activity of cytochrome *c* [20]. While stability and enzymatic activity of a few proteins in ionic liquid-containing aqueous media correlate with the Hofmeister's series [21,22] others do not [23,24]. Using simulations, it was also suggested that ionic liquids could influence xylanase activity by disturbing the dynamic motion of the protein in addition to affecting protein structure [25].

* Corresponding author. Current address: Department of Molecular, Cellular, and Biomedical Sciences, University of New Hampshire, Durham, NH 03824, USA.
E-mail address: krisztina.varga@unh.edu (K. Varga).
[1] Current address: Biomolecular Research Center, Boise State University, Boise, ID 83725, USA.

http://dx.doi.org/10.1016/j.bbrep.2016.08.009

Protein function is intimately linked to structure and dynamics, thus a molecular-based understanding of ionic liquid-protein interactions is vital for developing efficient applications. Recent studies [26,27] have demonstrated that solution NMR spectroscopy can be utilized to probe direct interactions between ionic liquids and proteins using NMR chemical shift perturbations, which are sensitive reporters of changes in the chemical environment, including protein structural changes. Kaar and coworkers [27] demonstrated interactions between [C_4-mim]Cl and lipase A at up to 0.29 M (*i.e.*, 5% v/v) ionic liquid, and Cabrita and coworkers [26] probed the interaction of various ionic liquids (up to 1 M concentration) with the protein Im. The results from these groups established that chemical shift perturbations in the 2D ^{1}H-^{15}N HSQC spectra could be used to monitor ionic liquid-induced structural changes in the proteins. It was suggested that both electrostatic as well as hydrophobic interactions occurred between proteins and ionic liquids, as a number of charged and nonpolar residues experienced chemical shift perturbations.

Although traditional solution state NMR techniques are applicable for relatively low ($\leq$ 1 M) concentrations of ionic liquids [26,27], the viscosity of the aqueous ionic liquid solutions above concentrations of 1 M are high enough to slow the tumbling of most proteins, thus sufficiently broadening NMR signals and limiting the use of solution state NMR. Importantly, several industrial and biomedical applications require high concentrations of ionic liquids. For example, ionic liquid-based pretreatment of biomass is being explored for removing lignin and hemicellulose under milder conditions than conventional acid or steam pretreatments [28], however the concentration of ionic liquids are fairly high (above 20% v/v) [28,29]. Another significant application of ionic liquids is to extend the life and quality of protein storage and formulation in the pharmaceutical industry; in these cases even higher concentrations of ionic liquids have been suggested for maintaining long-term maximal protein stability [17,30,31]. Thus, in order to probe ionic liquid–protein interactions at high ionic liquid concentration, pertinent to industrial applications, alternative NMR approaches that are not limited by slow tumbling are required.

High-resolution magic-angle-spinning (HR-MAS) NMR is particularly applicable for analyzing viscous or semi-solid samples using solution NMR methods while spinning at the magic angle in order to remove line-broadening effects. HR-MAS NMR has been shown to be a useful tool in monitoring chemical reactions [32] and in establishing the structure of small (e.g., $\leq$ 5 amino acids) peptides [33,34] in ionic liquids. HR-MAS reduces the line broadening caused by differences in magnetic susceptibly of the sample and also decreases the dipolar interaction and chemical shift anisotropy, although these effects are less significant in heterogeneous quasi-liquid samples [35].

Here, we demonstrate, for the first time, that a protein with $>$ 50 residues could be efficiently studied at atomic scale resolution in solution with high concentrations of ionic liquids using HR-MAS NMR. Specifically, structural and dynamical changes of the model 56-residue protein, immunoglobulin binding domain B1 of streptococcal protein G (GB1) [36] induced by a high concentration of [C_4-mim]Br (up to 3.5 M, which corresponds to 60%, v/v) were monitored by using 2D ^{1}H-^{15}N HSQC, 3D HNCA, and ^{15}N relaxation spectra of GB1. Significantly, the use of HR-MAS NMR spectroscopy surmounted the problem of line broadening due to the high viscosity of the ionic liquid-containing systems, and thus this technique could provide unique and precise information about site-specific ionic liquid–protein interactions. Arguably, this work provides an important foundation for probing protein secondary structure in ionic liquid-rich media.

2. Experimental

[C_4-mim]Br [37,38] and GB1 [39] were prepared as previously described. NMR samples were prepared by mixing a 4.4 mM GB1 stock solution in buffer (50 mM sodium phosphate, pH 5.50), D_2O, and neat [C_4-mim]Br in a pre-determined ratio to a 1.3 mM or 0.9 mM concentration of GB1 and a 10–50% v/v or 60% v/v final concentration of [C_4-mim]Br, respectively. Other samples included GB1 in 50% v/v glycerol/aqueous solution and 1.3 mM GB1 in the presence of 2.3 M KBr. A control GB1 sample was prepared without the addition of [C_4-mim]Br, KBr, or glycerol (referred to in the text as 0% v/v [C_4-mim]Br sample). HR-MAS NMR spectra were acquired on a 600 MHz Avance III Bruker NMR spectrometer equipped with a 4 mm HR-MAS probe at 27 °C and 5 kHz MAS frequency. Additional details are given in the SI.

3. Results and discussion

3.1. Selection of protein, ionic liquid, and experimental method

We probed the effects of [C_4-mim]Br on the protein GB1 to gain a better understanding of how ionic liquids impact protein structure, stability, and dynamics. The GB1 structure, folding pathway, and dynamics have been previously well characterized by NMR spectroscopy [40–44], which makes it an ideal model protein for assessment by HR-MAS spectroscopy. GB1 is a 56-residue stable protein comprised of one α-helix packed against a four-stranded β-sheet. 1-butyl-3-methylimidazolium bromide, [C_4-mim]Br, was chosen as a model ionic liquid, as it is a common, readily available, water-soluble, and widely used ionic liquid.

GB1 samples were prepared with varying concentrations of [C_4-mim]Br in NMR buffer: 0%, 10% (0.59 M), 25% (1.47 M), 40% (2.36 M), 50% (2.95 M), and 60% v/v (3.53 M) [C_4-mim]Br. To test the effects of high viscosity and high salt concentration media, control samples were also prepared in NMR buffer: GB1 in the presence of 50% glycerol and in the presence of 2.29 M KBr. A table describing the composition of each sample is given in Table S1. The HR-MAS NMR probe was configured for MAS and with a Z-axis gradient aligned along the magic angle to provide access to a wide range of solution NMR experiments. Significantly, using an HR-MAS probe allowed us to use deuterium lock and solvent suppression of the water signal using standard solution NMR pulse sequences. Although MAS induces large pressure especially on the sample near the inner wall of rotor, the low spinning frequency of 5 kHz in a 4 mm rotor did not destabilize GB1. A concentrated aqueous solution of GB1 was mixed with neat [C_4-mim]Br and D_2O, thus the ionic liquid concentration was limited by the minimum volumes of D_2O and protein solution. We acquired 1D ^{1}H, 1D ^{13}C, 2D ^{1}H-^{15}N HSQC, 3D HNCA, and ^{15}N relaxation spectra for GB1 utilizing HRMAS NMR. Although the VT inlet temperature was 27 °C under HRMAS condition, we estimated that the actual sample temperature was approximately 30–31 °C (due mostly to frictional heating) based on comparison of GB1 2D ^{1}H-^{15}N HSQC spectra under HR-MAS conditions to conventional solution GB1 2D ^{1}H-^{15}N HSQC spectra at various temperatures (Fig S1).

3.2. The effect of [C_4-mim]Br on the structure of GB1

1D ^{1}H spectra were not practical to detect changes in protein secondary structure due to the large excess of [C_4-mim]Br in solution (data not shown). Since GB1 was uniformly ^{15}N-, ^{13}C-enriched and [C_4-mim]Br was not, 1D ^{13}C spectra (Fig. S2) were utilized to monitor large changes in protein secondary structure in spite of the significant signal overlap, as discussed below. The [C_4-mim]Br signals were sharp, and their intensity

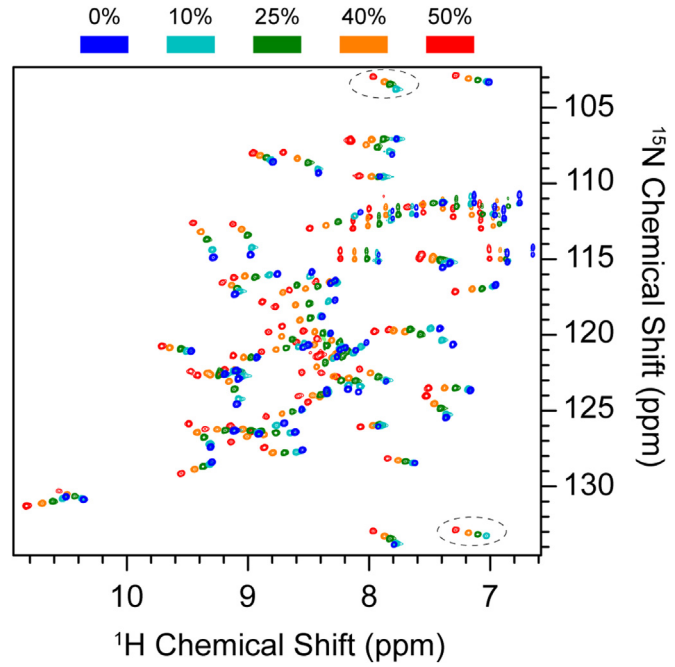

Fig. 1. 2D ^{1}H-^{15}N HSQC spectra of GB1 in the presence of [C_4-mim]Br. (a) Overlay of spectra with 0% (blue), 10% (cyan), 25% (green), 40% (orange), and 50% (red) v/v [C_4-mim]Br. Aliased peaks are shown in dashed ovals.

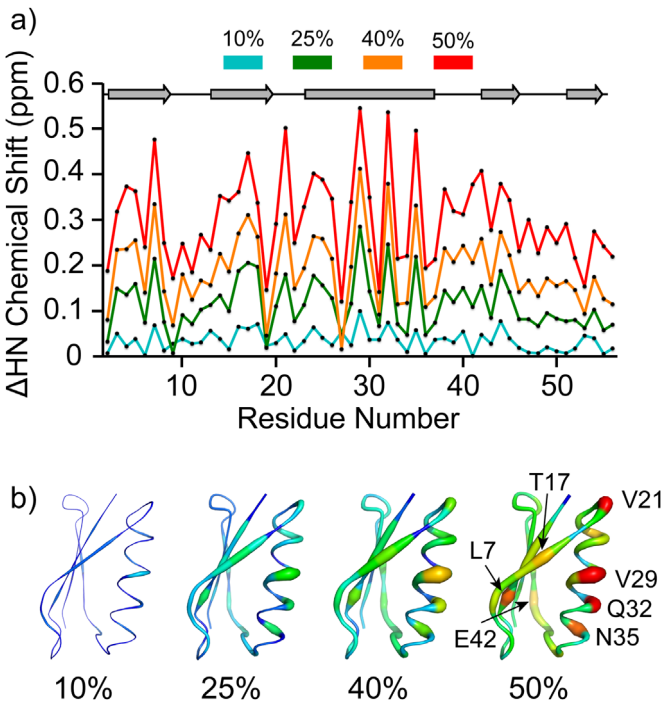

Fig. 2. Chemical shift perturbations for each residue in the presence of 10–50% v/v [C_4-mim]Br. (a) Combined and weighted ^{1}H and ^{15}N (ΔHN) chemical shift perturbations (CSP) of all residues in the presence of 10% (cyan), 25% (green), 40% (orange), 50% (red) v/v [C_4-mim]Br. (b) Cartoon representation of the crystal structure of GB1 (PDB: 2QMT) color coded by amide chemical shifts perturbation (CSP) in 10–50% v/v [C_4-mim]Br. Chemical shift perturbation is indicated by colors ranging from blue (least, 0.00 ppm) to red (most, 0.55 ppm), and the coloring gradient is scaled to the maximum CSP in the 50% [C_4-mim]Br sample. GB1 residues which have more 0.40 ppm CSP in the 50% v/v [C_4-mim]Br sample are identified. The maximum radius of the putty representation is scaled to maximum CSP in the shown condition (10% v/v [C_4-mim]Br, 25% v/v [C_4-mim]Br, 40% v/v [C_4-mim]Br or 50% v/v [C_4-mim]Br). The figure was generated by PYMOL.

increased as the ionic liquid concentration increased.

2D ^{1}H-^{15}N HSQC GB1 spectra were acquired for all GB1 samples, including GB1 in the presence of 0–60% v/v [C_4-mim]Br, 2.3 M KBr, and 50% v/v glycerol (Fig. 1 and Fig. S3). All 2D ^{1}H-^{15}N HSQC spectra were assigned based on published chemical shifts [41] and 3D HNCA spectra. 3D HNCA GB1 spectra were acquired for 0%, 10%, 25%, and 50% v/v [C_4-mim]Br and 2.29 M KBr samples. Fig. S4 shows the assigned ^{1}H-^{15}N HSQC spectra for GB1 in 0% [C_4-mim]Br, and Fig. S5 highlights examples of the HNCA strip plots used for assignments of the aqueous GB1 sample under HR-MAS conditions. The HNCA spectra were very well resolved even in the presence of 50% v/v [C_4-mim]Br, although the *i*-1 peak was often weak (Fig. S5c). 3D solution NMR methods under HR-MAS conditions could be a general tool for structural studies of biomacromolecules in viscous, high salt solutions.

Traditional solution NMR 2D ^{1}H-^{15}N HSQC spectra of GB1 in the presence of 50% v/v [C_4-mim]Br were acquired at both 600 and 900 MHz using cryogenically cooled probes (Fig S6). The quality of spectra from samples in solutions containing high concentrations of ionic liquids collected at high field with cryogen probes are often compromised by poor tuning and radiation damping thereby hindering traditional solution-based NMR experiments, especially when using cryogenically cooled probes (i.e., cryo/cold probes), [45] which are commonly used in protein NMR studies. In the case of GB1 in 50% v/v [C_4-mim]Br, the traditional solution NMR spectra were observed to have broader lines and T1 noise artifacts due to radiation damping (Fig S6 b,c). For example, G9 exhibited 23.0 Hz vs 33.9 Hz ^{1}H line width and L12 had a 32.86 Hz vs. 44.48 Hz ^{1}H line widths in the HRMAS vs. traditional solution NMR spectrum at 600 MHz. Further, radiation damping from 50% v/v [C_4-mim]Br results in significant noise at ca. 7.8 ppm and 9.1 ppm (Fig S6b,c), completely obscuring several GB1 peaks. Overall, the HR-MAS spectrum has a much better quality than the solution NMR spectrum.

High salt concentrations can induce perturbations in the protein amide ^{1}H and ^{15}N shifts due to a number of effects, including the bulk magnetic susceptibility of the solvent as well as interactions between the solvent and solute molecules [46]. Amide ^{1}H shifts in proteins are especially sensitive to hydrogen bonding [47] and can report on protein secondary structure changes. Therefore, we evaluated the chemical shift changes of the amide moieties in the backbone as a function of [C_4-mim]Br concentration using 2D ^{1}H-^{15}N HSQC. [C_4-mim]Br induced chemical shift changes in both the ^{1}H and ^{15}N dimensions (Figs. 1, 2, S3, and S7a,b). At 50% v/v [C_4-mim]Br, all GB1 residues showed a significant (0.10–0.54 ppm) downfield ^{1}H chemical shift perturbation. The ^{15}N chemical shift perturbations were more complex and not straightforward, ranging from −2.28 to 1.97 ppm at 50% v/v [C_4-mim]Br. The combined and weighted ^{1}H and ^{15}N chemical shift perturbations [47] (ΔHN) were calculated (Fig. 2a) using equation Eq. (S1). The large shift perturbations at high ionic concentrations indicated that the amino acid residue interactions with [C_4-mim]Br were significant along the protein backbone. The residues most affected (more than 0.40 ppm in ΔHN) by [C_4-mim]Br included L7, T17, V21, V29, Q32, N35, and E42 (Fig. 2b). In general, most amino acids with large chemical shift perturbations were nonpolar and charged polar residues. The anion, Br^-, is classified as a mild chaotrope (destabilizer) based on the Hofmeister's series. Bordusa and coworkers observed that neutral and chaotropic inorganic salts could cause significant chemical shift changes due to peptide-anion hydrogen bonding [34]. Thus, [C_4-mim]Br – protein interactions are likely driven by both hydrophobic and electrostatic forces. The largest chemical shift perturbations clustered to the α-helical region of

GB1. Additional evidence came from Cα chemical shift perturbations (known to be strong reporters of the protein's secondary structure), which were also significantly affected (ΔCα ranged from −0.21 to 1.05 ppm; Fig. S7c) by the increasing concentration of [C_4-mim]Br. Secondary structure predictions from 0, 25, and 50% IL were calculated using Talos+ (Table S4). An increase in loop content was found for residues K13, G14, and E15 and decrease in confidence of secondary structure assignment for residues in E42 and W43. K13, G14 and E15 are located near a turn previously identified as a melting hotspot in a destabilized mutant of GB1 [40].

At 60% v/v [C_4-mim]Br, GB1 exhibited multiple peaks in the ^{1}H-^{15}N HSQC for a number of residues and an increased number of peaks appeared in a narrow amide proton chemical shift at around 8.4–8.9 ppm (Fig. S3), which indicated the loss of homogeneous tertiary and secondary protein structure at 60% v/v [C_4-mim]Br. While some peaks shifted more downfield as anticipated based on our previously observed trends at lower concentrations (Fig. S3c), other additional peaks appear (Fig. S3d,e), implying the coexistence of a folded state and unfolded state of GB1.

Previous studies have shown that the thermal unfolding of GB1 is reversible throughout the transition between the folded and unfolded state [48,49]. To test whether the ionic liquid-induced unfolding was reversible, GB1 sample in 60% v/v [C_4-mim]Br was diluted with the buffer to obtain 40% v/v [C_4-mim]Br. Remarkably, the ^{1}H, ^{15}N spectrum of the resulting sample overlaid almost perfectly with the 40% v/v [C_4-mim]Br spectrum (Fig. S9b). In the ^{13}C 1D spectra, most individual amino acids were not well-resolved, however in the 60% v/v [C_4-mim]Br spectrum obvious changes were observed in the GB1 carbonyl region (Fig. S9a), which is a known sensitive reporter of protein secondary structure [50]. After the 60% v/v [C_4-mim]Br protein sample was diluted to 40% v/v [C_4-mim]Br, the carbonyl region displayed the characteristic profile of a 40% v/v [C_4-mim]Br-GB1 sample, consistent also with the observations in the ^{1}H, ^{15}N spectra. Overall, the data indicated that the unfolding of GB1 due to its interaction with [C_4-mim]Br was reversible, and the protein could re-gain its well defined native structure upon decreasing the ionic liquid content.

3.3. Molecular tumbling and backbone ^{15}N relaxation of GB1 in [C_4-mim]Br

Ionic liquids are much more viscous than most conventional solvents, and solution NMR measurements can be hindered by high viscosity. Although neat [C_4-mim]Br exhibited very high viscosity (i.e. 433 cP at 27 °C), the presence of water reduced the viscosity substantially (Table S5 and S10a). For instance, the viscosity of 60% v/v [C_4-mim]Br solution at 27 °C was 6.0 cP. For comparison, the viscosity of a 50% v/v glycerol in the NMR buffer was 8.4 cP, slightly higher than the viscosity of the 60% v/v [C_4-mim]Br mixture. The 2D ^{1}H-^{15}N HSQC spectrum of GB1 in 50% v/v glycerol appeared to be shifted upfield, while still being of similar resolution and quality as the GB1 spectrum without additives (Fig. S10b), thus the viscosity of the solution medium was not a major factor in protein destabilization.

Backbone ^{15}N spin relaxation T_1 and T_2 (from which R_1 and R_2 are calculated) were measured in order to determine the tumbling rates τ_c, for GB1 in 0%, 25%, and 50% aqueous [C_4-mim]Br. The residue specific R_1, R_2 and hetNOE relaxation data for 0% [C_4-mim]Br (Fig. S7d, S7e, S7f) supported previously published data of GB1 in solution state experiments [42], demonstrating that the HR-MAS technique did not introduce any observed, unintended effects. The average T_1 and T_2 values of the different solutions at the calculated τ_c values (Table 1) of 3.53 ns, 5.64 ns, and 10.37 ns for 0%, 25%, and 50% v/v [C_4-mim]Br were in good agreement with theoretical values (Fig. 3). In addition, they were

Table 1
^{15}N spin relaxation T_1 and T_2 and tumbling rate, τ_c of GB1-[C_4-mim]Br samples. The τ_c values were calculated from the ^{15}N NMR data (relax) or based on Stoke's Law (SL), as described in detail in the Supplemental information. IL stands for ionic liquid.

Sample	Ave. T_1/ms	Ave. T_2/ms	τ_c, relax /ns	τ_c, SL /ns
0% IL	160.6	377.1	3.53	3.46
25% IL	103.7	436.2	5.64	5.88
50% IL	62.9	721.1	10.37	13.27

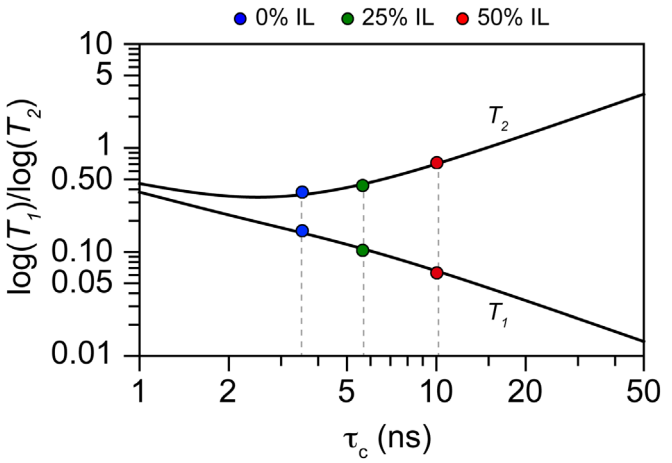

Fig. 3. Rotational correlation times (τ_c) for GB1 in 10%, 25% and 50% v/v [C_4-mim]Br. Rotational correlation times were calculated from an average of T_1 and T_2 times of non-flexible residues for GB1 in the presence of 0% (blue), 25% (green), and 50% (red) v/v [C_4-mim]Br. The theoretical T_1 and T_2 curves were calculated using a home written Mathematica script. IL stands for ionic liquid.

in a relatively good agreement with values calculated using Stoke's law (Eq. (S2) and (S3).), especially at lower viscosities. Although GB1 is a small model protein which tumbles reasonably well even in high viscosity solvents, our results show that the HR-MAS technique can be utilized as an alternative technique to traditional solution NMR to study proteins in high concentrations of ionic liquids, which will be particularly advantageous when applied to large proteins.

The residue specific R_1 and R_2 are sensitive reporters of the ps-ns timescale motions and can be used to measure the backbone motions of a protein. At 25% and 50% v/v [C_4-mim]Br, GB1 showed a relative decrease in R_1 and increase in R_2 rates for residues 20–30, which were found in the N-terminal half of the α-helix, and consistent with previous findings that suggest that the N-terminal part of the helix was part of an unfolding hotspot [40]. These ^{15}N relaxation results support the chemical shift data, which suggests that higher concentrations of [C_4-mim]Br destabilize and promote local unfolding of GB1.

In conclusion, we have demonstrated that HR-MAS NMR spectroscopy is a viable tool to study atomic level protein–ionic liquid interactions in a high ionic liquid concentration (3.53 M), high inorganic salt concentration (2.29 M), and high viscosity (7.4 cP). Specifically, the chemical shift perturbation analysis of ΔHN and ΔCα suggested that the α-helical region of GB1 had the strongest interaction with [C_4-mim]Br. Interestingly, even though regions of the protein with the highest CSP did not appear to change their secondary structure dramatically even in 50% ionic liquid, where it is clear that in 60% v/v [C_4-mim]Br, GB1 folded and unfolded states coexisted. However, GB1 unfolding was reversible upon dilution to 40% [C_4-mim]Br. Residue specific R_1, R_2 and het-NOE relaxation data obtained for GB1 in the presence of 0%, 25%, and 50% v/v [C_4-mim]Br show that the protein not only

experiences decreased tumbling rates due to viscosity, but also shows changes in the ps-ns timeframe consistent with destabilization of a previously reported unfolding hotspot. The GB1 tumbling rates in [C_4-mim]Br solutions were in good agreement with theoretical values, thus supporting the use of HR-MAS as a tool for studying proteins or large molecules in highly viscous and high ionic strength media. Importantly, the results of this study open up many exciting possibilities for further structural and dynamical characterization of other, in high concentration of ionic liquids, which will advance the fundamental understanding of how ionic liquids influence native protein secondary structure and function, a critical step in the development of many applications.

Acknowledgments

This work was supported by the National Science Foundation (awards CHE-1413696, CBET-1403947, and DGE-0948027), by the U.S. Department of Energy under Contract No. DE-AC36-08-GO28308 with the National Renewable Energy Laboratory, and by the University of Wyoming. The BioEnergy Science Center is a U.S. Department of Energy Bioenergy Research Center supported by the Office of Biological and Environmental Research in the DOE Office of Science. The research was partially supported by Institutional Development Awards (IDeA) from the National Institute of General Medical Sciences of the National Institutes of Health under Grants P20GM103432 (KV and SEF), P20GM103408 (LW) and P20GM109095 (LW). We thank Chad M. Rienstra at the University of Illinois at Urbana-Champaign for generously providing the GB1 sample.

Transparency document. Supplementary material

Transparency document associated with this article can be found in the online version at http://dx.doi.org/10.1016/j.bbrep.2016.08.009.

Appendix A. Supplementary material

Supplementary data associated with this article can be found in the online version at http://dx.doi.org/10.1016/j.bbrep.2016.08.009.

References

[1] J.P. Hallett, T. Welton, Room-temperature ionic liquids: solvents for synthesis and catalysis. 2, Chem. Rev. 111 (2011) 3508–3576.
[2] F. van Rantwijk, R.A. Sheldon, Biocatalysis in ionic liquids, Chem. Rev. 107 (2007) 2757–2785.
[3] E. Santos, J. Albo, A. Irabien, Magnetic ionic liquids: synthesis, properties and applications, RSC Adv. 4 (2014) 40008–40018.
[4] M.A. Neouze, M. Kronstein, F. Tielens, Ionic nanoparticle networks: development and perspectives in the landscape of ionic liquid based materials, Chem. Commun. 50 (2014) 10929–10936.
[5] M.G. Ma, J.F. Zhu, Y.J. Zhu, R.C. Sun, The microwave-assisted ionic-liquid method: a promising methodology in nanomaterials, Chem.: Asian J. 9 (2014) 2378–2391.
[6] G. Gebresilassie Eshetu, M. Armand, B. Scrosati, S. Passerini, Energy storage materials synthesized from ionic liquids, Angew. Chem. Int. Ed. 53 (2014) 13342–13359.
[7] M. Kar, T.J. Simons, M. Forsyth, D.R. MacFarlane, Ionic liquid electrolytes as a platform for rechargeable metal-air batteries: a perspective, Phys. Chem. Chem. Phys. 16 (2014) 18658–18674.
[8] D.R. MacFarlane, N. Tachikawa, M. Forsyth, J.M. Pringle, P.C. Howlett, G. D. Elliott, J.H. Davis, M. Watanabe, P. Simon, C.A. Angell, Energy applications of ionic liquids, Energy Environ. Sci. 7 (2014) 232–250.
[9] Y. Medina-Gonzalez, S. Camy, J.-S. Condoret, $ScCO_2$/green solvents: biphasic promising systems for cleaner chemicals manufacturing, ACS Sustain. Chem. Eng. 2 (2014) 2623–2636.
[10] R. Abro, A.A. Abdeltawab, S.S. Al-Deyab, G. Yu, A.B. Qazi, S. Gao, X. Chen, A review of extractive desulfurization of fuel oils using ionic liquids, RSC Adv. 4 (2014) 35302–35317.
[11] G. Cevasco, C. Chiappe, Are ionic liquids a proper solution to current environmental challenges? Green Chem. 16 (2014) 2375–2385.
[12] C.P. Kapnissi-Christodoulou, I.J. Stavrou, M.C. Mavroudi, Chiral ionic liquids in chromatographic and electrophoretic separations, J. Chromatogr. A 1363 (2014) 2–10.
[13] T. Payagala, D.W. Armstrong, Chiral ionic liquids: a compendium of syntheses and applications (2005–2012), Chirality 24 (2012) 17–53.
[14] L.P. Jameson, J.D. Kimball, Z. Gryczynski, M. Balaz, S.V. Dzyuba, Effect of ionic liquids on the conformation of a porphyrin-based viscometer, RSC Adv. 3 (2013) 18300–18304.
[15] L.P. Jameson, S.V. Dzyuba, Ionic liquid-controlled conformational bias of tetracycline, RSC Adv. 3 (2013) 4582–4587.
[16] L.P. Jameson, S.V. Dzyuba, Circular dichroism studies on intermolecular interactions of amphotericin b in ionic liquid-rich environments, Chirality 25 (2013) 427–432.
[17] N. Byrne, L.-M. Wang, J.-P. Belieres, C.A. Angell, Reversible folding-unfolding, aggregation protection, and multi-year stabilization, in high concentration protein solutions, using ionic liquids, Chem. Commun. (2007) 2714–2716.
[18] M. Bihari, T.P. Russell, D.A. Hoagland, Dissolution and dissolved state of cytochrome c in a neat, hydrophilic ionic liquid, Biomacromolecules 11 (2010) 2944–2948.
[19] G.A. Baker, W.T. Heller, Small-angle neutron scattering studies of model protein denaturation in aqueous solutions of the ionic liquid 1-butyl-3-methylimidazolium chloride, Chem. Eng. J. 147 (2009) 6–12.
[20] P. Bharmoria, T.J. Trivedi, A. Pabbathi, A. Samanta, A. Kumar, Ionic liquid-induced all-[small alpha] to [small alpha]+[small beta] conformational transition in cytochrome c with improved peroxidase activity in aqueous medium, Phys. Chem. Chem. Phys. 17 (2015) 10189–10199.
[21] D. Constantinescu, H. Weingärtner, C. Herrmann, Protein denaturation by ionic liquids and the Hofmeister series: a case study of aqueous solutions of ribonuclease A, Angew. Chem. Int. Ed. 46 (2007) 8887–8889.
[22] J.-Q. Lai, Z. Li, Y.-H. Lu, Z. Yang, Specific ion effects of ionic liquids on enzyme activity and stability, Green Chem. 13 (2011) 1860–1868.
[23] Z. Yang, Y.-J. Yue, W.-C. Huang, X.-M. Zhuang, Z.-T. Chen, M. Xing, Importance of the ionic nature of ionic liquids in affecting enzyme performance, J. Biochem. 145 (2009) 355–364.
[24] A. Kumar, P. Venkatesu, Does the stability of proteins in ionic liquids obey the Hofmeister series? Int. J. Biol. Macromol. 63 (2014) 244–253.
[25] V.W. Jaeger, J. Pfaendtner, Structure, dynamics, and activity of xylanase solvated in binary mixtures of ionic liquid and water, ACS Chem. Biol. 8 (2013) 1179–1186.
[26] A.M. Figueiredo, J. Sardinha, G.R. Moore, E.J. Cabrita, Protein destabilisation in ionic liquids: the role of preferential interactions in denaturation, Phys. Chem. Chem. Phys. 15 (2013) 19632–19643.
[27] E.M. Nordwald, G.S. Armstrong, J.L. Kaar, NMR-guided rational engineering of an ionic-liquid-tolerant lipase, ACS Catal. 4 (2014) 4057–4064.
[28] A. Brandt, J. Grasvik, J.P. Hallett, T. Welton, Deconstruction of lignocellulosic biomass with ionic liquids, Green Chem. 15 (2013) 550–583.
[29] C. Li, B. Knierim, C. Manisseri, R. Arora, H.V. Scheller, M. Auer, K.P. Vogel, B. A. Simmons, S. Singh, Comparison of dilute acid and ionic liquid pretreatment of switchgrass: biomass recalcitrance, delignification and enzymatic saccharification, Bioresour. Technol. 101 (2010) 4900–4906.
[30] K. Fujita, M. Forsyth, D.R. MacFarlane, R.W. Reid, G.D. Eiliott, Unexpected improvement in stability and utility of cytochrome c by solution in biocompatible ionic liquids, Biotechnol. Bioeng. 94 (2006) 1209–1213.
[31] N.M. Micaelo, C.M. Soares, Protein structure and dynamics in ionic liquids. Insights from molecular dynamics simulation studies, J. Phys. Chem. B 112 (2008) 2566–2572.
[32] A. Rencurosi, L. Lay, G. Russo, D. Prosperi, L. Poletti, E. Caneva, HRMAS NMR analysis in neat ionic liquids: a powerful tool to investigate complex organic molecules and monitor chemical reactions, Green Chem. 9 (2007) 216–218.
[33] C. Mrestani-Klaus, A. Richardt, C. Wespe, A. Stark, E. Humpfer, F. Bordusa, Structural studies on ionic liquid/water/peptide systems by HR-MAS NMR spectroscopy, ChemPhysChem 13 (2012) 1836–1844.
[34] A. Richardt, C. Mrestani-Klaus, F. Bordusa, Impact of ionic liquids on the structure of peptides proved by HR-MAS NMR spectroscopy, J. Mol. Liq. 192 (2014) 9–18.
[35] K. Elbayed, B. Dillmann, J. Raya, M. Piotto, F. Engelke, Field modulation effects induced by sample spinning: application to high-resolution magic angle spinning NMR, J. Magn. Reson. 174 (2005) 2–26.
[36] A. Gronenborn, D. Filpula, N. Essig, A. Achari, M. Whitlow, P. Wingfield, G. Clore, A novel, highly stable fold of the immunoglobulin binding domain of streptococcal protein G, Science 253 (1991) 657–661.
[37] S.V. Dzyuba, K.D. Kollar, S.S. Sabnis, Synthesis of imidazolium room-temperature ionic liquids. Exploring green chemistry and click chemistry paradigms in undergraduate organic chemistry laboratory, J. Chem. Educ. 86 (2009) 856–858.
[38] S.V. Dzyuba, R.A. Bartsch, Efficient synthesis of 1-alkyl(aralkyl)−3-methyl (ethyl)imidazolium halides: precursors for room-temperature ionic liquids, J. Heterocycl. Chem. 38 (2001) 265–268.
[39] W.T. Franks, D.H. Zhou, B.J. Wylie, B.G. Money, D.T. Graesser, H.L. Frericks, G. Sahota, C.M. Rienstra, Magic-angle spinning solid-state NMR spectroscopy of the beta 1 immunoglobulin binding domain of protein G (GB1): N-15 and

C-13 chemical shift assignments and conformational analysis, J. Am. Chem. Soc. 127 (2005) 12291–12305.
[40] K.Y. Ding, J.M. Louis, A.M. Gronenborn, Insights into conformation and dynamics of protein GB1 during folding and unfolding by NMR, J. Mol. Biol. 335 (2004) 1299–1307.
[41] D.J. Wilton, R.B. Tunnicliffe, Y.O. Kamatari, K. Akasaka, M.P. Williamson, Pressure-induced changes in the solution structure of the GB1 domain of protein G, Proteins: Struct. Funct. Bioinform. 71 (2008) 1432–1440.
[42] D. Idiyatullin, I. Nesmelova, V.A. Daragan, K.H. Mayo, Heat capacities and a snapshot of the energy landscape in protein GB1 from the pre-denaturation temperature dependence of backbone NH nanosecond fluctuations, J. Mol. Biol. 325 (2003) 149–162.
[43] J.H. Tomlinson, M.P. Williamson, Amide temperature coefficients in the protein G B1 domain, J. Biomol. NMR 52 (2012) 57–64.
[44] M.K. Frank, G.M. Clore, A.M. Gronenborn, Structural and dynamic characterization of the urea denatured state of the immunoglobulin binding domain of streptococcal protein G by multidimensional heteronuclear NMR spectroscopy, Protein Sci. 4 (1995) 2605–2615.
[45] A.E. Kelly, H.D. Ou, R. Withers, V. Dotsch, Low-conductivity buffers for high-sensitivity NMR measurements, J. Am. Chem. Soc. 124 (2002) 12013–12019.
[46] P. Kukic, F. O'Meara, C. Hewage, J.E. Nielsen, Coupled effect of salt and pH on proteins probed with NMR spectroscopy, Chem. Phys. Lett. 579 (2013) 114–121.
[47] M.P. Williamson, Using chemical shift perturbation to characterise ligand binding, Prog. Nucl. Magn. Reson. Spectosc. 73 (2013) 1–16.
[48] P. Alexander, S. Fahnestock, T. Lee, J. Orban, P. Bryan, Thermodynamic analysis of the folding of the streptococcal protein-G IgG-binding domains B1 and B2 - why small proteins tend to have high denaturation temperatures, Biochemistry 31 (1992) 3597–3603.
[49] H.P. Chiu, B. Kokona, R. Fairman, R.P. Cheng, Effect of highly fluorinated amino acids on protein stability at a solvent-exposed position on an internal strand of protein G B1 domain, J. Am. Chem. Soc. 131 (2009) 13192–13193.
[50] J. Yao, H.J. Dyson, P.E. Wright, Chemical shift dispersion and secondary structure prediction in unfolded and partly folded proteins, FEBS Lett. 419 (1997) 285–289.